Effective Medium Theory Applied to Colloidal Solution of Gold Nanoparticles and Alternating Gold-Silica Multilayer Thin Film Composites

[1]ZAHEER ABBAS KHAN, [2]RACHANA KUMAR AND [3]JOYDEEP DUTTA

[1]*P.O.Box 1021, Optics labs, Islamabad, Pakistan.*
[2]*Center of Excellence in Nanotechnology, School of Engineering and Technology, Asian Institute of Technology, Klong Luang, Pathumthani 12120, Thailand.*
Currently, Associate Professor, Kalindi College, University of Delhi.
[3]*Chair in Nanotechnology, Water Research Center, Sultan Qaboos University,*
123 Al-Khoudh, Sultanate of Oman.
engrzak@gmail.com*

Summary: Optical modeling of multilayer thin films constructed with oppositely charged nanoparticles help us to understand phenomenon such as surface plasmon resonance, absorbance, transmittance and reflectance. This work reports the application of Maxwell-Garnett effective medium theory in quasi-static limit to colloidal suspensions consisting of host material silica and the inclusion material -gold nanoparticles. Layer-by-layer deposition method was used to self-assemble these nanoparticles to build multilayer composite films. By varying the number and thickness of the layers and the size and spacing of the metal inclusion, a facilitative optical design is modeled to build multilayers of nanosized materials targeted for desired applications.

Keywords: Maxwell-Garnett, layer-by-layer, gold, silica, nanoparticles

Introduction

We are now at the threshold of a revolution in the ways which materials and products are created. This is due to the convergence of the traditional fields of physics, mathematics, chemistry and engineering to form a new field of nanotechnology- particles in the size range of nanometers [1, 2]. At this very small scale, important new properties are exhibited that differ radically from those of the bulk form-new properties that significantly improve performance of materials and devices [3-5]. Nanotechnology has been established in a broad range of diverse fields that includes synthesis and processing of nanoparticles and materials, self-assembly techniques, fabrication of unique nanostructures, supramolecular chemistry and the exploitation of quantum effects [6-8].

There are two generalized approaches for making nanomaterials– top-down and bottom-up [9, 10]. In the top-down approach, bulk materials are transformed into nanoscale materials by microelectronic fabrication techniques, ball milling, electro-erosion processes, etc. The bottom-up approach, emphasized in this paper, is the synthesis of nanoscale materials from atoms and molecules. The latter process has vast potential for future applications due to its simplicity with capability to tailor design specific structure and function– similar to the way nature accomplishes its remarkable processes [11, 12]. The potential for high throughput and facilitative scale up are also attractive from the bottom-up perspective. Molecular self-assembly is one of the most significant bottom-up approaches and is considered to be a promising fabrication method in nanotechnology [13, 14]. This method is defined as the spontaneous formation of complex hierarchical structures from pre-designed building blocks without excessive input of energy or direction from an outside source. It is the spontaneous aggregation of molecules under equilibrium conditions joined together, for the most part, with non-covalent bonds [15].

Multilayer thin film synthesis based on layer-by-layer self-assembly of nanoparticles is relatively a new method of thin film growth [16, 17]. One variation employs charged polyelectrolytes and oppositely charged nanoparticles that are alternately deposited to form the multilayered structure. There are many advantages to this method. First of all, the process is very simple and requires neither hardware nor restricted environmental control. Secondly, the deposition technique results in layers that are highly homogeneous. Lastly, we can use layer-by-layer assembly to combine nanoparticles with other functional materials, such as dyes, proteins and DNA, to create functional nanostructured materials with greater complexity [18-20].

The optical properties of nanoscale materials are different from their large scales counterparts [21, 22]. Optical modeling of multilayer thin films constructed with a dielectric and oppositely charged nanoparticles helps us understand phenomena such as the surface plasmon resonance absorption, reflectivity, transmittance, and scattering and, for

---

*To whom all correspondence should be addressed.

example, the mechanisms that govern the electronic states of diodes constructed by this method. We can then predict the behavior of multilayer thin film in which the number of layers and thickness of each layer satisfies a specific application intended to use as an optical or electronic device [23, 24].

Effective medium theory is a method of treating macroscopic non-homogeneous media in which properties such as the conductivity σ and dielectric function ε vary in space [25]. The composite consists of a host material *h* (usually a transparent insulator) and an inclusion material *i* (usually a nanometal) [26, 27]. J.C. Maxwell-Garnett introduced the first effective medium theory in the early 1900s [28]. The Maxwell-Garnett (MG) model is based on several assumptions: 1. Inclusion particles are isotropic and uniform in size; 2. The radius of the inclusion metal 'r_i' is assumed to be much smaller than the spacing between inclusions; and 3. The inclusion radius is much smaller than the wavelength 'λ' of the incident radiation. The latter defines the case of the quasi-static limit in which r_i << 0.01 λ [29]. The propagation of light is described by effective (composite) values of the optical constants of the inclusion, host and composite. The specific complex dielectric function 'ε' is derived from the optical constants– e.g. the refractive index '*n*' and the absorption coefficient '*k*' of the material where $\varepsilon = n - ik$. Thus, for the effective optical response of the composite material, the Maxwell-Garnett expression is given by [30]:

$$\frac{\varepsilon_{eff} - \varepsilon_h}{\varepsilon_{eff} + 2\varepsilon_h} = f_i \left(\frac{\varepsilon_i - \varepsilon_h}{\varepsilon_i + 2\varepsilon_m} \right) \qquad (1)$$

where 'ε_{eff}', 'ε_i' and 'ε_h' are the complex dielectric functions of the composite, metal inclusion and host materials respectively and 'f_i' is the volume fraction of the metal nanoparticle inclusion. The number '2' appearing in the denominator is a shape-dependent parameter that is specific for spheres [31].

MG simulation was applied to model the metal inclusion (colloidal gold(Au) nanoparticle) in a host medium (water). The volume fraction of spherical gold nanoparticles with an average diameter of 20 nm was varied in the range (0.01 < f_i < 0.25) and the effects of change in volume fraction on the optical absorbance spectra were studied. Another model was developed for the composite layered thin films of gold nanoparticles alternated with cationic *polymer* (*poly*(diallyldimethylammoniumchloride, *PDDA*) capped silica nanoparticles. Multi-layered

composites consisting of alternating layers of negatively charged Au layers (~ 20 nm diameter) and positively charged silica nanoparticles (~ 30 nm) were evaluated for their optical response for different number of layers ranging from 25 to 100.

Experimental

Layer-by-layer (LBL) structures consist of three components: 1. clean activated glass substrates, 2. citrate-stabilized gold colloids with overall negative charge, and 3. PDDA-capped silica nanoparticles with overall positive charge. Bare glass substrates (ca. 2 cm² area) were cleaned and activated in hot piranha solution (a mixture v:v of 4:1 H_2SO_4 and H_2O_2 respectively). The treatment enhances the hydrophilicity of the surface by increasing the population of hydroxyl [–OH] groups that also serve as binding sites for subsequent attachment [32, 33]. Chemical modification was achieved by application of the silane 3-aminopropyl–trimethoxysilane (APTS) in 95% methanol. At pH 10, the silanized surface layer acquired a negative charge [34].

Colloid Preparation:

Citrate stabilized gold nanoparticles colloid was prepared by boiling a mixture of chloroauric acid [$HAuCl_4$] and trisodium citrate [$Na_3(C_6H_5O_7)$] according to a modified method of Turkevtich et al and others [35, 36]. Attainment of the diagnostic ruby colored solution indicated the presence of gold colloids ca. 20 nm in diameter. Silica nanoparticles were prepared by Stober process involving hydrolysis and polycondensation of tetraethyl orthosilicate (TEOS) in ethanol [37]. Initially, 100 ml of ethanol was mixed with 40 ml of deionised (DI) water and 18 ml of TEOS (99.99%) and sonicated about 30 minutes at temperature 35°C. Then 14 ml of ammonia solution (25%) (NH_4OH) was mixed with 14 ml of DI water. This solution was added drop wise to TEOS mixture under constant stirring. Finally a grey solution appears showing the formation of Silica nanoparticles. Centrifuged the final solution at 4000 rpm for 20 minutes and collected the supernatant. Then equal volume of DI water was added to this solution and heated at 90°C to evaporate the ethanol for phase transformation. Silica nanoparticles thus produced, bear a negative charge. The average size of Silica nanoparticles obtained by this method is around 30 nm. Later, 0.558ml of PDDA (35%) was added to the solution and stirred for 30 minutes. PDDA capped silica nanoparticles thus produced, bear a positive charge.

Multi-Layer Film Fabrication

Multi-layered thin films were fabricated using the directed self-organization of colloidal nanoparticles [38, 39]. Layer-by-layer (LBL) growth of gold-polyelectrolyte layers was accomplished via sequential adsorption of positively charged PDDA capped silica and negatively charged citrate stabilized Au nanoparticle colloids. The cationic PDDA capped silica and anionic citrate stabilized gold contributed to the electrostatic interaction between monolayers to form layered structures. The activated substrate was first dipped in saturated PDDA capped silica and rinsed with DI water and relative pH buffer to form a monolayer. Following rinsing, the first layer was dipped into the negatively charged Au colloid solution. The duration of each dipping step was 5 min followed by air dry for another 5 minutes. The cycle (ca. 40 minutes) was repeated until the desired number of layers was attained Fig. 1.
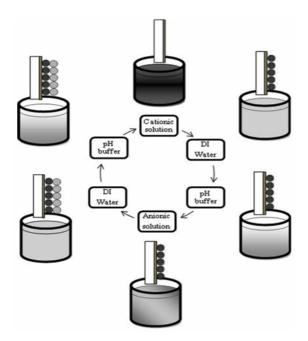

Fig. 1: Illustration of the layer-by-layer deposition process.

Characterisation Procedures:

The optical absorption spectra of the colloidal solution of gold nanoparticles and multilayered thin films were taken using USB 4000-FLG diode array spectrometer (Ocean optics Co. Ltd., Dunedin, FL). the optical measurements were carried out in the UV-VIS wavelength range of 200-1100 nm using the light source of tungsten halogen lamp (Micropack Co. Ltd., Ostfildern, Germany). Particle size distribution of the gold nanopartciles in the colloidal solutions was calculated from the electronic micrographs using ImageJ® software. Transmission electron micrographs (TEM) of colloidal gold and silica nanoparticle solutions were taken with TEM (JEOL-JEN2010) operating at 200KV. Scanning electron micrographs (SEM) of the top and crossectional view of gold-silica multilayer films were taken using SEM (JEOL JSM-6301F) operating at 20KV.

Simulations:

Optical modeling was accomplished with SCOUT® (Wolfgang Theiss, Aachen, Germany) simulation software. MG optical absorbance spectra were simulated for colloidal gold nanoparticles (~ 20 nm) in water (host medium) with varying volume fraction $0.01 < f_{Au} < 0.25$. Similarly MG simulations were performed for optical absorbance spectra of multilayers of gold nanoparticles (~ 20 nm) embedded with PDDA capped silica nanoparticles (~ 30 nm) (host medium) for different number of bi-layers. Optical parameters fitting were carried out to adjust simulated and measured data using the dielectric constants of the Au nanoparticles [40].

Results and Discussion

Spherical gold nanoparticles were synthesized with a particle size around 20 nm for the purpose to neglect the scattering effects so that the extinction is only due to the dipole absorption which results from surface plasmon resonance of Au nanoparticles. Particle size distribution based on the transmission electron micrograph confirmed that mean particle size of gold nanoparticles is 20 nm that are uniformly dispersed in the water medium Fig 2a. Electrostatic stabilization of the colloidal solution of gold nanoparticles is achieved by an electrical double layer arising from the mutual repulsion among the charged nanoparticles. Similarly spherical silica nanoparticles were synthesized with a particle size around 30 nm to maintain the size compatibility with the gold nanoparticles for the fabrication of gold-silica multilayered film. Transmission electron micrograph confirmed the uniform dispersion of colloidal silica nanoparticles with a mean particle size of 30 nm Fig. 2b. Steric stabilization in the colloidal solution of silica nanoparticles is realized by binding of polymer (PDDA) surfactant molecules to the surface of silica nanoparticles. The long chains of the organic molecules prevent the nanoparticles from coming close to each other due to osmotic repulsion, thus provides the colloidal stability to the solution.
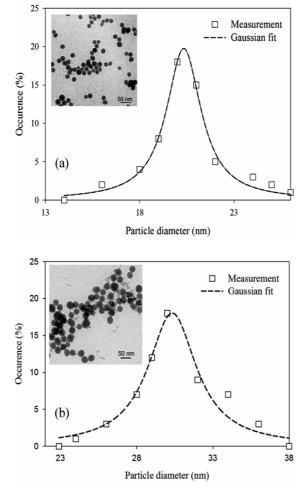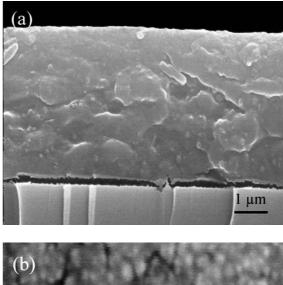
Fig. 2: (a) Particle size distribution with the gaussian fit shows an average particle size ~ 20 nm from the transmission electron micrograph of gold nanoparticles (inset). (b) Particle size distribution with the gaussian fit shows an average particle size ~ 30 nm from the transmission electron micrograph of silica nanoparticles (inset).
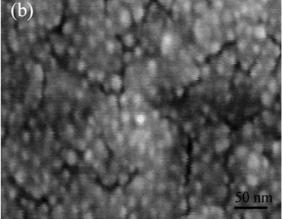
Fig. 3: (a) Scanning electron micrograph of the crossection of a multilayered thin film consisting of 100 bi-layers of gold nanoparticles (~ 20 nm) with alternate layers of silica nanoparticles (~ 30 nm). (b) Scanning electron micrograph showing gold nanoparticles as the top layer of the multilayer thin film Fig. 3(a).

Multilayers of gold nanoparticles were uniformly deposited on the glass substrate using the alternate layers of PDDA capped silica nanoparticles resulting in a stack of individual self-assembled particle layers as shown in the scanning electron micrograph Fig. 3a. Densely packed gold nanoparticles in the top layer of the multilayer thin film show the successful formation of individual layers however there is a minimum spacing among the nanoparticles due to the random sequential absorption of few layers that reduced the final surface coverage Fig. 3b.

MG Simulations of Au-Water Composites with Variations in Volume Fraction:

Optical extinction spectra based on the MG model was simulated for gold nanoparticles of 20 nm suspended in water. The water ($n = 1.33$) served as the host material of the metal-host composite [41]. The volume fraction was varied from $0.01 < f_i < 0.25$ and the simulated optical absorbance spectra is presented Fig. 4a. Similarly the wet-chemical synthesis of colloidal gold nanoparticle was carried out with different set of solution having volume fractions 0.01, 0.05, 0.1 and 0.25. The experimental

values of optical extinction spectra were taken for all set of solutions and results are displayed in Fig. 4.2b.
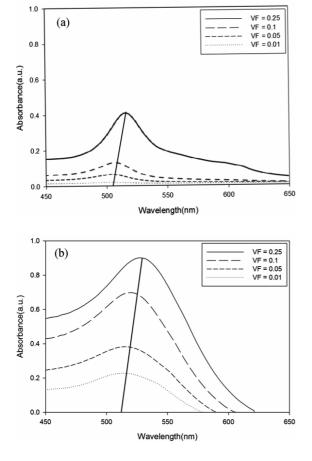

Fig. 4: (a) MG simulated optical absorbance spectra of colloidal gold nanoparticles (~ 20 nm) in water (host medium) with varying volume fraction $0.01 < f_{Au} < 0.25$. (b) Experimental optical absorbance spectra of colloidal gold nanoparticles (~ 20 nm) in water (host medium) with varying volume fraction $0.01 < f_{Au} < 0.25$.

Two trends are noticeable. First, there is an increase in signal intensity as f_i is increased. The increase in intensity is simply due to the presence of more material. Secondly, there is an apparent red shift in λ_{max} with increasing f_i. Moreover, a clear shift to longer wavelengths of λ_{max} is observed when $f_{Au} > 0.05$. A straightforward physical explanation follows.

The red shift in λ_{max} can also be explained mathematically. From the MG formula we get:

$$(\varepsilon_{eff} - \varepsilon_h)(\varepsilon_i + 2\varepsilon_h) = f_i(\varepsilon_i - \varepsilon_h)(\varepsilon_{eff} + 2\varepsilon_h) \qquad (2)$$

$$\varepsilon_{eff}[(\varepsilon_i + 2\varepsilon_h) - f_i(\varepsilon_i - \varepsilon_h)] = f_i(\varepsilon_{eff} + 2\varepsilon_h) + \varepsilon_h(\varepsilon_i + 2\varepsilon_h) \quad (3)$$

$$\varepsilon_{eff} = \varepsilon_h \frac{\varepsilon_i(1 + 2 f_i) + \varepsilon_h(1 - f_i)}{\varepsilon_i(1 - f_i) + \varepsilon_h(2 + f_i)} \qquad (4)$$

The dielectric constant of a metal is complex, thus:

$$\varepsilon_i(\lambda) = \varepsilon_i^{/}(\lambda) + i.\varepsilon_i^{//}(\lambda) \qquad (5)$$

where $\varepsilon_i^{/}(\lambda)$ is the real part and $\varepsilon_i^{//}(\lambda)$ is the imaginary part of the complex dielectric function of the metal. Therefore, a maximum in absorption is observed at the wavelength that satisfies the following condition:

$$\varepsilon_i^{/}(\lambda) = -\frac{2 + f}{1 - f}\varepsilon_h \qquad (6)$$

If $f_i \ll 1$, we get the condition for maximum absorption for the dipolar plasmon resonance for spherical nanoparticles:

$$\varepsilon_i^{/}(\lambda) = -2\varepsilon_h \qquad (7)$$

Defining a function $G(f_i)$:

$$G(f_i) = \frac{2 + f_i}{1 - f_i} = 2 + \frac{3}{\frac{1}{f_i} - f_i} \qquad (8)$$

When the volume fraction f_i increases, then $\left(\frac{1}{f_i} - 1\right)$ decreases and $G(f_i)$ increases. This leads to a decrease of $\varepsilon_i^{/}(\lambda)$ at the peak wavelength. Correlations with the reported real part of the dielectric function of gold, Au $[\varepsilon_i^{/}(\lambda)]$ show that this model is plausible, i.e. that $\varepsilon_i^{/}(\lambda)$ decreases with increasing wavelength of incident light in both cases. Scattering effects were minimized for this simulation by keeping the size of Au nanoparticles confined to 20 nm. Extinction, therefore, is assumed to be due solely to the dipolar resonance condition of the surface plasmon.

A red shift in λ_{max} is noted at the wavelength of maximum absorption (at the left top ends of the spectra). The broadness of the profiles indicates that the impact of the gold fraction is greater in the case of the BG condition than it is for the MG condition.

MG Simulations of Au-SiO₂ Composites with Variations in Number of layers

Simulations for the optical absorbance spectra of the metal-dielectric matrix were carried out

for the multilayered structure. The gold-silica composite consisting of individual layers of gold nanoparticles (~ 20 nm) with alternate layers of silica nanoparticles (~ 30 nm) were modeled based on the MG theory. The numbers of layers were varied from 25 to 100 and results are shown in Fig. 5a. There is no appearant shift in the peak values of the optical spectra as the simulations assume that gold nanoparticles are perfectly sized and the resultant layers are uniformly deposited that forms a homogeneous layered structure.
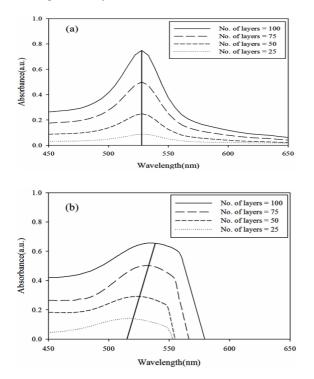

Fig. 5: (a) MG simulated optical absorbance spectra of multilayers of gold nanoparticles (~ 20 nm) embedded with PDDA capped silica nanoparticles (~ 30 nm) (host medium) for different number of bi-layers. (b) Experimental optical absorbance spectra of multilayers of gold nanoparticles (~ 20 nm) embedded with PDDA capped silica nanoparticles (~ 30 nm) (host medium) for different number of bi-layers.

However the experimental values of the optical extinction spectra for the different number of multilayer i.e. 25, 50, 75 and 100, showed a red peak shift Fig. 5b. In the multilayered thin film composites, with the mean size of Au nanoparticles held at 20 nm, the distance d_{Au} between nanoparticles is reduced as number of layers is increased. With reduction in d_{Au}, electronic interactions between nanoparticles are enhanced by close proximity to form induced dipolar interactions (e.g. polarizations). Such coupling of surface plasmons with nearest neighbors relaxes electronic states overall by enhancing polarizability of conduction band electrons. The delocalization results in a shift to lower energy absorption– e.g. a red shift in λ_{max}.

Conclusions

Colloidal gold nanoparticles (ca.20 nm) embedded in silica dielectric matrix (ca.30 nm) were evaluated for their optical response. An increase in signal intensity was observed as volume fraction of gold colloid is increased. In addition there is an apparent red shift in peak wavelength with increasing volume fraction. With Au nanoparticles size fixed at 20 nm the distance between nanoparticles is reduced as volume fraction is increased. The coupling of surface plasmons with neighbors relaxes electronic states by increasing the polarizability of conduction band electrons. The delocalization results in lower energy absorption or a red shift in peak wavelength. Films made of gold nanoparticles embedded in silica dielectric matrix were evaluated for their optical response using Maxwell-Garnett (MG) theory. An increase in maximum absorption was also observed with increasing the number of deposition cycles. This can be attributed to increase in absolute film mass of multilayered structures with increasing number of bilayers. In the experimental spectra a small red shift in wavelength is observed with increase in number of layers. This effect is attributed to the random sequential absorption of gold nanoparticles to build multilayers and the interparticle plasmon coupling within the layers.

References

1. G. Lovestam, H. Rauscher, G. Roebben, B. Sokull Klüttgen, N. Gibson, J. P. Putaud and H. Stamm, *JRC Reference Report, EUR 24403 EN*, 1 (2010).

2. K. R. Schmidt*, Project on Emerging Nanotechnologies 6,* Woodrow Wilson International Center for Scholars*,* Washington DC (2007).

3. P. R. Westmoreland, *Chemical Engineering Progress*, **104**, 30 (2008).

4. R. W. Murray, *Chemical. Reviews*, **108**, 2688 (2008).

5. G. Shen and D. Chen*, Science of Advanced Materials*, **1**, 213 (2009).

6. G. Tegart, *Proceedings of the Second International Conference on Technology Foresight*, Tokyo, Japan, p.1 (2003).

7. C. N. R. Rao, A. Muller and A. K. Cheetham, *the Chemistry of Nanomaterials: Synthesis, Properties and Applications, (Eds.:*C. N. R. Rao*, A. Muller, A. K. Cheetham)* WILEY-VCH, Weinheim, Germany, p.1 (2004).

8. A. Umar, M. S. Akhtar, S. H. Kim, A. Al-Hajry, M. S. Chauhan and S. Chauhan, *Science of Advanced Materials*, **3**, 695 (2011).

9. M. F. Ashby, P. J. S. G. Ferreira and D. L. Schodek, *Nanomaterials*, *Nanotechnologies and Design : An Introduction for Engineers and Architects*, Butterworth-Heinemann, Oxford, UK, p.5 (2009).

10. R. Psaro, M. Sgobba and M. Guidotti, Inorganic and Bio-inorganic Chemistry II, *Encyclopedia of life Support Systems*, UNESCO, p.1 (2004).

11. N. J. Guido, X. Wang, D. Adalsteinsson, D. McMillen, J. Hasty, C. R. Cantor, T. C. Elston and J. J. Collins, *Nature*, **439**, 856 (2006).

12. W. Lu and C. M. Lieber, *Nature Materials*, **6**, 841 (2007).

13. J. Ouellette, Harvard University, *The Industrial Physicist, American Institute of Physics*, p.26 (2000).

14. L. C. Palmer and S. I. Stupp, *Accounts of Chemical Research*, **41**, 1674 (2008).

15. G. L. Hornyak, J. Dutta, H. F. Tibbals and A. K. Rao, *Introduction to Nanoscience*, CRC Press, Florida, p.613 (2008).

16. N. A. Kotov and L. M. Liz-Marzán, *Nanoscale Materials, L. M. Liz-Marzán and P. V. Kamat (eds.)*, Kluwer Academic, p.273 (2003).

17. X. F. Su, X. F., Kim, B. S, S. R. Kim, P. T. Hammond and D. J. Irvine, *ACS Nano*, **3**, 3719 (2009).

18. E. M. Saurer, C. M. Jewell, J. M. Kuchenreuther and D. M. Lynn, *Acta Biomaterialia*, **5**, 913 (2009).

19. Q. Zhao and B. Li, *Nanomedicine: Nanotechnology, Biology and Medicine*, **4**, 302 (2008).

20. B. Masereel, M. Dinguizli, C. Bouzin, N. Moniotte, O. Feron, B. Gallez, B, T. V. Borght, C. Michiels and S. Lucas, *Journal of Nanoparticle Research*, **13**, 1573 (2011).

21. P. C. Ray, *Chemical Reviews*, **110**, 533 (2011).

22. A. Carne, C. Carbonell, I. Imaz and D. Maspoch, *Chemical Society Reviews*, **40**, 291 (2011).

23. S. H. M Jafri, J. Dutta, D. Sweatman and A. B. Sharma, *Applied Physics Letters,* **89,** 133123 (2006).

24. Z. A. Khan, R. Kumar, W. S. Mohammed, G. L. Hornyak and J. Dutta, *Journal of Materials Science*, **46**, 6877 (2011).

25. D. Stroud, The *Effective Medium Approximation, Superlattices and Microstructures*, Academic Press, New York, USA, **23**, 3/4, p.567 (1998).

26. R. Kitsomboonloha, C. Ngambenjawong, W. S. Mohammed, M. B. Chaudhari, G. L. Hornyak and J. Dutta, *Micro and Nano Letters*, IET**, 6,** 342 (2011).

27. J. S. Ahn, P. T. Hammond, M. F. Rubner and I. Lee, *Colloids and Surfaces* A, **259**, 45 (2005).

28. J. C. Maxwell-Garnett, *Proceedings of the Philosphical Transactions Research Society*, London, U. K., **203**, p.385 (1904).

29. S. G. Coulson, *Monthly Notices of Royal Astronomical Society*, **389**, 1885 (2008).

30. D. E. Aspnes, *American Journal of Physics*, **50**, 704 (1980).

31. Jr. C. A. Foss, G. L. Hornyak, J. A. Stockert and C. R. Martin, *Journal of Physical Chemistry*, **98,** 2963 (1994).

32. H. H. Hinterwirth, M. Strobl and H. Al-Dubai, *Chemical Monthly,* **141**, 291 (2010).

33. R. Benters, C. M. Niemeyer, D. Drutschmann, B. Blohm and D. Wohrle, *Nucleic Acids Research*, **30**, E10 (2002).

34. S. Promnimit and J. Dutta, *Journal of Nano Research*, **11**, 1 (2010).

35. J. Turkevich, P. C. Stevenson and J. Hillier, *Discussions of Faraday Society*, **11**, 55 (1951).

36. S. H. M. Jafri, A. B. Sharma, C. Thanachayanont and J. Dutta, *MRS 2005 fall meeting*, Boston, MA. Rb18.1 (2005).

37. W. Stober, A. Fink and E. Bohn, *Journal of Colloid and Interface Science,* **26**, 62 (1968).

38. S. Promnimit, C. Cavelius, S. Mathur and J. Dutta, *Physica* E, **41**, 285 (2008).

39. Z. Adamczyk, P. Weroński and J. Barbasz, *Journal of Colloid Interface Science*, **317**, 1 (2008).

40. E. D. Palik, *Handbook of Optical Constants of Solids III*, Academic Press, New York (1998).

41. N. Nath and A. Chilkoti, *Analytical Chemistry*, **74,** 504 (2002).